Extended Abstracts of the 1997 International Conference on Solid State Devices and Materials, Hamamatsu, 1997, pp. 456-459

Invited

Current Status of 200 mm and 300 mm Silicon Wafers

Howard R. Huff and D. W. McCormack, Jr.
SEMATECH, 2706 Montopolis Drive, Austin, TX 78741
and
Chi Au, Troy Messina, Kevin Chan and Randal K. Goodall
I300I, 2706 Montopolis Drive, Austin, TX 78741

1. Introduction

Experimental data for particles, metals and flatness, based on a recent analysis of 200 mm epitaxial wafers from 7 global silicon suppliers, are presented extending similar analyses for 150 mm polished[1)] and 200 mm epitaxial wafers[2)]. These data are useful for comparison with current data for 300 mm developmental wafers to identify opportunities for cost-effective improvements in 300 mm wafers. Since the initial oxygen content ($O_i°$) was not specified for these 300 mm wafers, the opportunity to assess oxygen precipitation on 300 mm sectioned wafers over a wide range of $O_i°$ values will also be presented.

2. 200 mm Epitaxial Wafers

Each supplier provided one cassette of 25 p/p^+ (100) 3-5 µm epitaxial wafers randomly sampled from lots targeted for "leading edge" customers (c. 1996). Each supplier was given a unique code letter. Suppler B provided 4 cassettes of wafers; suppliers A and D each provided 2 cassettes of wafers, the latter differing principally in the substrate thermal process prior to epitaxial deposition.

Particles. Localized Light Scatterers (LLS) were measured on a Tencor 6200 calibrated to PSL spheres[3)]. Due to the absence of crystal originated pits (COPs) in the epitaxial films, LLS counts are reported as "particles ≥ size." The box plot in Figure 1 indicates most suppliers constrained particles to ≤ 50/wafer (6 mm edge exclusion, EE) for diameter ≥ 0.125 µm (0.18/cm^2) while similar data were also obtained for 3 mm EE, corresponding to 0.17/cm^2.

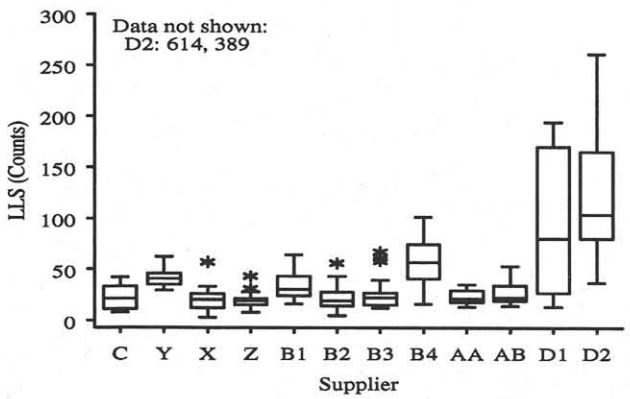

Figure 1. Dependence of Localized Light Scatterers (LLS) with Supplier (LLS ≥ 0.125 µm, 6 mm edge exclusion)

Metals. Metallic contamination by Fe, Ni, Cu, Zn as well as Ca, Cl and S were measured by TXRF using a Rigaku 3720; 3 data were taken for each of 22 wafers (center and 80 mm from the center at Θ = 125° and Θ = 325° (notch at 270°). Similar data were obtained by a 9-point sampling pattern for 3 wafers. The box plot for 66 Fe data per supplier in Figure 2 indicates their capability of constraining Fe (and similarly Ni, Cu and Zn) to the "effective" detection limit of about 1-2 x 10^{10}/cm^2. Data for Ca, Cl and S will also be presented.

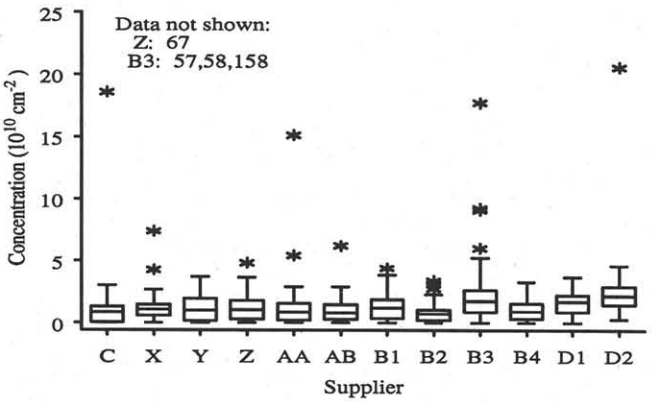

Figure 2. Dependence of Surface Fe with Supplier

Flatness. Wafer dimensional information was obtained using an ADE 9300. Most suppliers constrained global front-surface least squares reference plane total indicator range (GFLR)[4)] ≤ 1.5 µm, total thickness variation (GBIR)[4)] ≤ 2.5 µm, bow between -14 and +10 µm and warp between 10 and 40 µm. The larger warp value, for suppliers with a back-surface oxide, is relaxed during IC thermal processing.

Most suppliers' constrained the total indicator range flatness, based on a front-surface site least squares reference plane (SFQR)[4)], to ≤ 0.20 µm for 25 mm x 25 mm complete sites with 3 suppliers ≤ 0.13 µm. Inclusion of the 25 partial sites somewhat degrades these values as seen by comparing the 32 complete sites with the 25 partial sites in the box plot of Figure 3. A detailed comparison of the ratio of SFQD[4)] to SFQR indicated a range of 0.58-0.65, comparable to previous data[1,2)] and consistent with a recent model[5)].

Microroughness. All suppliers constrained micro-roughness (R_q) values to approximately ≤ 1.0 Å and 1.5 Å for scan sizes of 1 x 1 and 20 x 20 µm, respectively. Crystal lattice terraces, previously observed on vicinal (100) epitaxial wafers[6)] were generally not observed on these wafers.

3. 300 mm Polished Wafers

Initial particle, metal and flatness data for 300 mm polished wafers indicate that individual parameter data comparable with state-of-the-art 200 mm wafers can be achieved. The

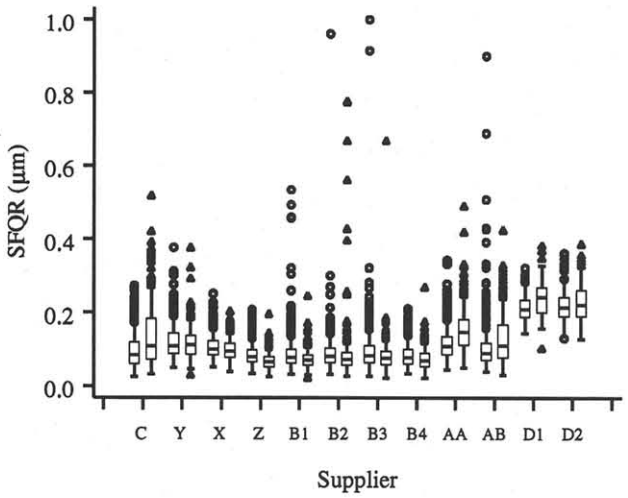

Figure 3 Dependence of SFQR with Supplier
(Complete Sites = o and Partial Sites = Δ)

utilization of a wire saw for cutting 300 mm wafers resulted in comparable bow and warp data. Double-side polishing resulted in encouraging SFQR data for several suppliers while other suppliers still have immature polishing processes. A steep gradient in the learning curve is being pursued by all suppliers. Continued improvements in controlling the magnitude, tolerance and uniformity of silicon wafer parametrics is essential, consistent with the requirement of balancing the "best wafer possible" against the cost-of-ownership (CoO) opportunity of not driving silicon requirements to the detection limit but to some less stringent and optimized value[7].

Oxygen Precipitation. Two 300 mm wafers from each of 4 suppliers were measured for O_i°, by the intensity of the 1107 cm^{-1} line on a Bio-Rad Map 300. A total of 13 O_i° measurements were taken along the whole diameter for each wafer with a 4 mm EE to assess the radial homogeneity. Carbon, measured by the 605 cm^{-1} line, was generally about 0.03 ppma for all suppliers except supplier C (≈ 0.1 ppma). Each wafer was subsequently quartered and re-measured for O_i° radially. The change in O_i ($\Delta O_i = O_i^\circ - O_i^f$) was determined following ASTM Standards procedures[8] (i.e., a one-step 16 hr anneal at 1050C and a two-step 16 hr anneal at 1050C following a 4 hr nucleation pre-anneal at 750C). The samples remained in the furnace as the temperature was ramped 10C/min from 750C to 1050C. Post-test O_i^f were obtained in regions spatially close to the original readings.

Since none of the wafers received the conventional thermal donor anneal by the supplier (due to the unavailability of a 300 mm furnace at the time of wafer preparation), the influence of both a 450C, 2 hr anneal to generate additional thermal donors and a 625C, 30 min anneal to annihilate thermal donors was also examined. Neither thermal process materially resulted in a change in ΔO_i. This is not surprising, however, since the short range restructuring in these cases does not significantly perturb O_i°, inasmuch as O_i°, approximately 1.25 - 1.80 x $10^{18}/cm^3$ (25-36 ppma) utilizing the "old" ASTM relation between intensity and concentration, is about 1000x the number of thermal donors.

The 1050C, 16 hr anneal did not result in any significant precipitation, even for samples with O_i° about 36 ppma (see Figure 4a). However, the samples which received the donor anneal at 625C plus the 1050C thermal process exhibited significant oxygen precipitation for O_i° beyond 36 ppma as seen in Figure 4b. It appears the donor anneal facilitates the formation of nuclei which accelerates oxygen precipitation at 1050C for sufficiently high O_i°. The utilization of the 750C, 4 hr nucleation anneal prior to the 1050C, 16 hr thermal process in Figure 4c, however, exhibited an accelerated oxygen precipitation and the familiar "s-shaped curve." This is not unexepected since 700-800C is optimal for the formation of nuclei[9] to facilitate oxygen precipitation at 1050C. The three step process of 625C followed by 750C and 1050C exhibited similar behavior (see Figure 4d). These ΔO_i data approach an O_i^f value approximately equal to 12 ppma, compared to the thermal equilibrium solid solubility value of 8.5 ppma at 1050C[10]. Previous tests perfomed in 1996 exhibited faster precipitation inasmuch as those 300 mm sectioned wafers came from crystals that were larger than the throat of the 200 mm crystal puller and were held within the chamber as the crystal cooled down, presumably generating sufficient numbers of nuclei facilitating oxygen precipitation, even for the one-step ASTM test[11].

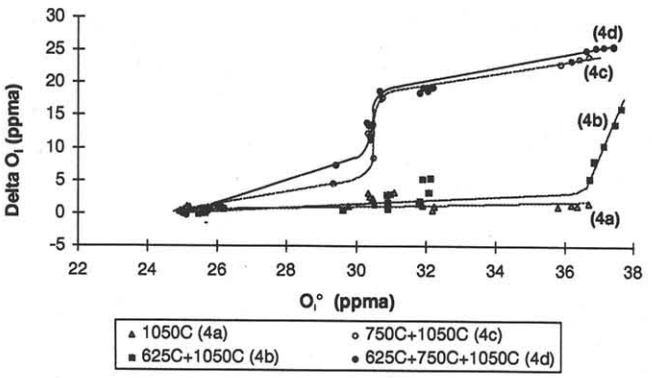

Figure 4. Delta Interstitial Oxygen vs. Initial Interstitial Oxygen

In order to gain further insight into the oxygen precipitation kinetics with $O_i^\circ \approx 25$, 30, 32 and 36 ppma, a series of tests varied the 750C nucleation time from 0-64 hrs as well as assessed the influence of an RTA anneal at 750C, 30s as an alternative to the conventional 650C, 30min thermal donor anneal. All the sections then received the 1050C precipitation anneal for times varying from 0-99 hrs. The fraction of oxygen precipitated is described by eq. 1:

$$\xi \equiv [O_i^\circ - O_i^f(t)] / [O_i^\circ - O_i^{eq}] \qquad (1)$$

The 1050C precipitation test generally exhibited a monotonic and steeper gradient in ξ with increasing nucleation anneal times of 4, 16 and 64 hrs at 750C for $O_i^\circ \geq$ 30 ppma as seen in Figure 5 (O_i° = 32 ppma). The curves

Continued on the 575 page

saturate around 16 hrs and, for a pre-anneal time of 64 hrs, approaches O_i^{eq} of 8.5 ppma.

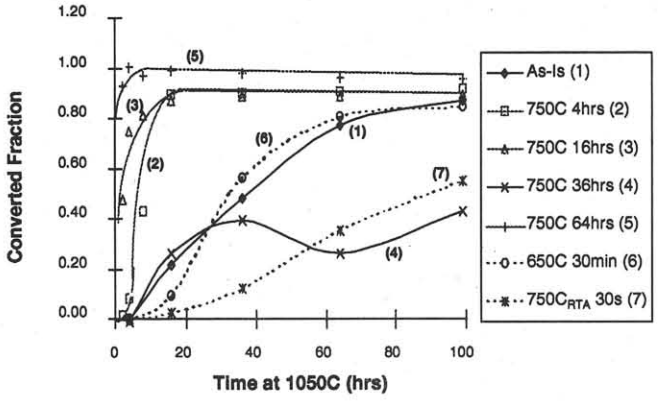

Figure 5. O_i Converted Fraction: Supplier C (O_i° = 32 ppma)

The 750C, 36 hr nucleation samples exhibited a retardation in ξ, increasing with increased O_i°, which appears consistent, in principle, with previous three-inch crystal experimental data[12]. This phenomenon has been explained in terms of the dissolution of nuclei during the 1050C growth temperature due to the 36 hr 750C anneal generating an elastic strain in the crystal due to the growth of SiO_2 nuclei which is thermally relaxed by an SiO_2 polymorph change and the emission of silicon interstitials at 1050C which drives the oxygen precipitation reaction backwards[13,14]. Annealing for 64 hrs at 750C for $O_i^\circ \geq 30$ ppma, however, produces sufficient crystal strain to generate silicon interstitials even at 750C which, if exceeding a critical limit, collapse into dislocation loops. Subsequent oxygen precipitation at 1050C, therefore, recovers from the retardation phenomenon since the dislocation loops act as a readily available sink to capture emitted interstitials due to further SiO_2 polymorph changes at 1050C and the availability of a sufficiently sized nuclei distribution density facilitating the approach to O_i^{eq}.

The characterization of the time dependence of the oxygen precipitation is described in eq. 2 by the Avrami relation[15]:

$$\xi = 1 - \exp[-kt^n] \qquad (2)$$

where n and k are constants characteristic of the precipitation kinetics. Figure 6 illustrates the variation of $\ln(\ln(1-\xi)^{-1})$ versus ln (t) at 1050C for O_i° = 32 ppma with the nucleation time at 750C as a parameter as well as the 650C thermal donor anneal and the 750C 30s RTA anneal.

The 650C anneal and 750C nucleation anneals exhibited no change in O_i° except for on supplier which had a $\Delta O_i \approx 4$ ppma for an $O_i^\circ \approx 32$ ppma for 64 hrs at 750C. The sections which received a 650C anneal or no anneal exhibited rather similar precipitation behavior for $O_i^\circ \approx 25$, 30 and 32 ppma at 1050C. For $O_i^\circ \approx 36$ ppma, the 650C anneal (no anneal) sections showed a steeper increase (significant decrease) in ΔO_i relative to $O_i^\circ \approx 32$ ppma. The 650C anneal approaches the 750C pre-anneal behavior (for 4, 16 and 64 hrs) for 99 hr at 1050C in Figure 5. The 750C, 30s RTA anneal exhibited larger ΔO_i for O_i° = 30 ppma and smaller ΔO_i for

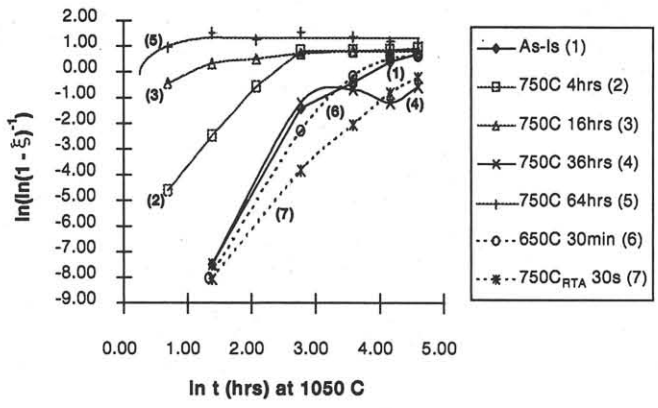

Figure 6. Avrami Analysis: Supplier C (O_i° = 32 ppma)

$O_i^\circ \approx 32$ ppma, compared to both the 650C anneal and no anneal at 1050C (see Figure 5) and also exhibited a further decrease in ΔO_i at $O_i^\circ \approx 36$ ppma, similar to the no anneal case. Indeed, the 750C, 30s anneal exhibited decreasing ΔO_i with $O_i^\circ > 30$ ppma. Clearly, further experimental and theoretical work is required for clarification of these observations.

4. Conclusion

Encouraging characterization data for 300 mm wafers has been obtained, indicating individual parameter data in some cases comparable to state-of-the-art 200 mm wafers. Initial oxygen precipitation data in 300 mm sectioned wafers indicates behavior consistent with previously observed phenomenon. Extensive further work is required for further clarification and detailed comparison to 200 mm behavior.

Acknowledgements

We appreciate the assistance of Carolyn F.H. Gondran, Jesse Santos, Emily Morales and Chris Sparks in facilitating the 200 mm data measurements and Billy Nguyen and Darryl Cheek in facilitating the thermal processing of the 300 mm pieces sectioned by Jon Crabtree.

References

1) H.R. Huff et al., J. Electrochem. Soc.,140, 229 (1993)
2) H.R. Huff et al., ECS Ext. Abst., 95-1, 269 (1995)
3) H.R. Huff, R.K. Goodall, et al., J.Electrochem. Soc., 144, 243 (1997)
4) *SEMI Int'l Stds.* 1994 - Materials M1-96, 20 (1996)
5) R.K. Goodall and H.R. Huff, SPIE 2725, 76-85 (1996)
6) Y.E. Strausser et al., ECS Ext. Abst. 94-1,461(1994)
7) H.R. Huff and R.K. Goodall, *Semi. Char.*, 67 (1996) AIP Press
8) *ASTM Stds.*, F 1239-94, 10.05, Electronics II, (1997)
9) N. Inoue et al., *Semconductor Silicon/1981*, 282 (1981)
10) E. Wijaranakula, Appl. Phys. Letts., 59, 1185 (1983)
11) H.R. Huff et al., *ULSI/97*, 135 (1997)
12) C.Y. Kung et al., *Defects in Silicon*, 185 (1983)
13) T.Y. Tan and C.Y. Kung, J. Appl. Phys., 59, 917 (1986)
14) J.-Y. Huh et al., J. Appl. Phys., 77, 5563 (1995)
15) J.W. Christian, *The Theory of Transformations in Metals and Alloys*, Pergamon Press (1965)

Continued from the 457 page